

Synthesis and Surface Relief Gratings of Three-Armed Star-Shaped Molecules Bearing 4-(*N,N*-Diphenyl)Amino-4'-Nitroazobenzene Chromophores

Jung Eun Lee, Kyung Moon Jung, Min Ju Cho, Kyung Hwan Kim, and Dong Hoon Choi*

Department of Chemistry, Advanced Materials Chemistry Research center, Korea University, Seoul 136-701, Korea

Received December 9, 2007; Revised January 26, 2008; Accepted January 28, 2008

Abstract: Three-armed, star-shaped molecules containing 4-(*N,N*-diphenyl)amino-4'-nitroazobenzene chromophores were synthesized to study the diffraction behavior after inscribing surface relief gratings. The two molecules differed in terms of their mode of chromophore attachment to the core. In compound **5**, they were bound to the core laterally through alkylene spacers, whereas the chromophores were tethered perpendicularly to the core in compound **4**. Although 60 wt% of the polar azobenzene chromophores was comprised of large molecules, no aggregation behavior was observed in the absorption spectra of the thin films. The surface relief gratings were elaborated on the surface of the molecular films by the two-beam interference method. The dynamics of grating formation were studied in terms of the diffraction efficiency using two different film samples made up of two star-shaped molecules. The maximum diffraction efficiency of D-(ENAZ)₃, compound **4**, was measured to be about 30%, which was significantly high. The mode of chromophore attachment affected the dynamic properties of the diffraction gratings.

Keywords: azobenzene chromophore, star-shaped molecules, surface relief grating, photoisomerization.

Introduction

There has been a considerable interest in the synthesis and characterization of azobenzene containing polymers to possess unique optical properties.¹⁻⁵ The optical data storage and holographic applications are still attractive topics for these photosensitive materials. Optically induced anisotropy in an azobenzene-containing polymer is a very promising intrinsic property needed for optical information storage and erasing. The mechanism of writing information involves photoinduced excitation of the azobenzene group, which undergoes *trans-cis-trans* isomerization. The mechanism of surface relief grating (SRG) also includes photo-induced molecular reorientation and mass transfer of azobenzene moieties.

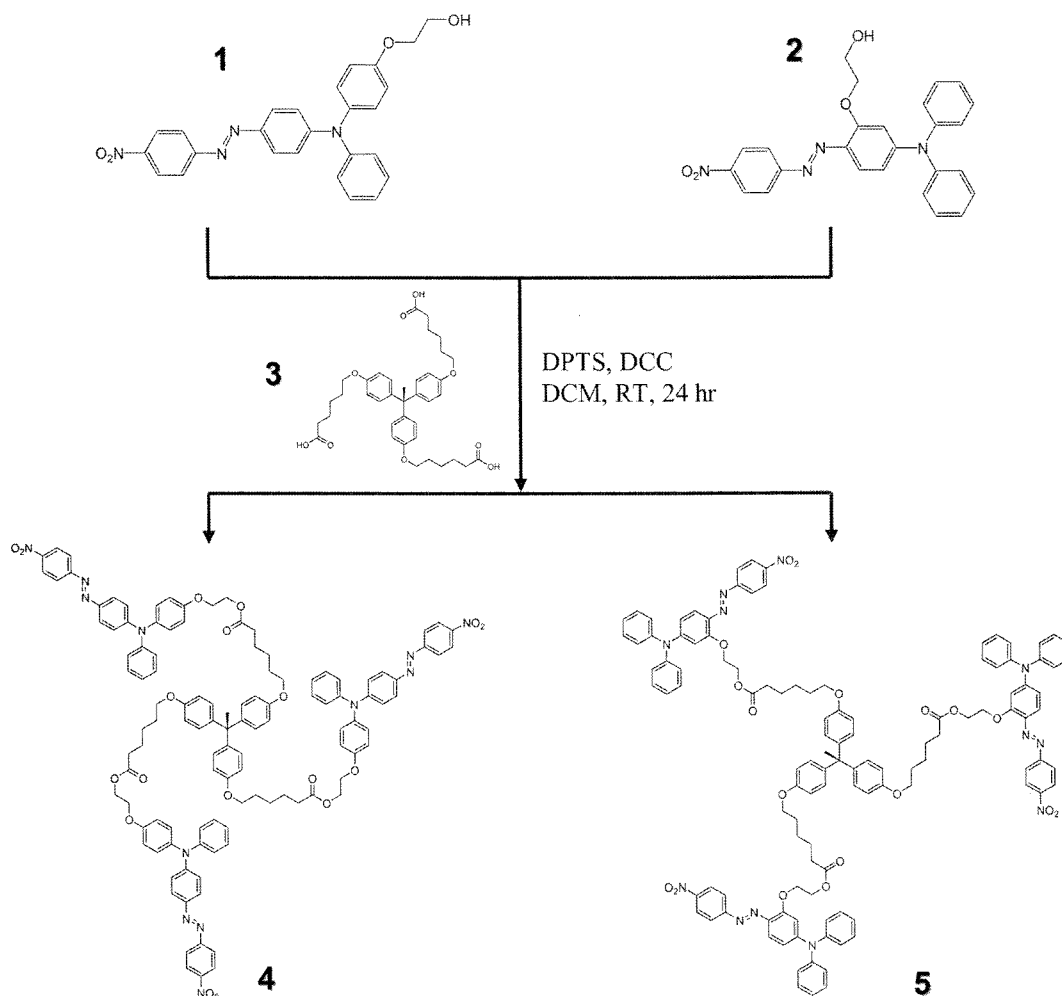
Two-beam interference on the polymer surface drove dramatic change of the optical properties in the localized area of a thin or thick film. Erasable gratings formed in the films of azobenzene-containing polymers have been studied extensively since they were first reported by Todorov *et al.*⁶⁻⁹ Both side chain and main chain azo-polymers have been investigated for various grating formations.¹⁰⁻¹⁶ All the polymers that show efficient surface relief gratings reported to date were polymers containing azobenzene chromophores in their side chains. SRGs recorded on these polymers are stable when kept below the glass transition temperature (T_g).

The patterns can be erased optically even below T_g or by heating the samples above T_g .

When we consider the possibility to utilize the azobenzene containing polymer for optical information storage by laser assisted holographic grating formation, the diffraction efficiency is the essential parameter to be maximized for high performance of devices. In general, the azobenzene containing polymer did show relatively low diffraction efficiency compared to the other local responsive photopolymers. The azobenzene elastomers developed by A. Bai *et al.* were demonstrated to be side chain liquid crystalline polymers and they showed efficient surface relief grating behaviors, which result in a fairly high diffraction efficiency of around 10-13%.¹⁷ P. Rochon *et al.* synthesized polyurethanes whose main chains contain azobenzene units. They also showed very high diffraction efficiency ($\eta=22-23\%$) that has not reported until then.¹⁸ Recently, the azobenzene functionalized polyimide showed quite high diffraction efficiency of 33-35% with the intensity of the excitation light and the kinetics was studied in detail with variable parameters.¹⁹

In order to establish a relationship between the molecular structure and the value of induced diffraction efficiency, we synthesized two different star-shaped molecules carrying the 4-(*N,N*-diphenyl)amino-4'-nitroazobenzene chromophore attached to the core unit either in an end-on (**4**) or a side-on (**5**) fashion (see Scheme I). We report on the properties of

*Corresponding Author. E-mail: dhchoi8803@korea.ac.kr



Scheme I. Synthetic route to three-armed star-shaped molecules containing 4-(*N,N*-diphenyl)amino-4'-nitroazobenzene chromophores.

these molecules for fabricating the diffraction grating controlled by a coupled linearly polarized ($\pm 45^\circ$) visible lights ($\lambda = 514$ nm). The effect of binding mode on the dynamic properties of the diffraction efficiency was investigated using the exposed films of two molecules below T_g . The dynamics of diffraction grating formation was studied in terms of the variation of the diffraction efficiency. Also, the erasing behavior of the gratings was examined under the irradiation of a linearly polarized single beam. According to the mode of attachment of azobenzene-chromophore to the core, we could investigate the different dynamic properties of the diffraction efficiency.

Experimental

4-(*N,N*-diphenyl)amino-4'-nitroazobenzene chromophores such as **1** and **2** were synthesized, following our previous method.²⁰

Synthesis.

Synthesis of Tris(2-(4-((4-((*E*)-(4-nitrophenyl)diazenyl)phenyl)(phenyl)amino)phenoxy)ethyl)-6,6',6''-(4,4',4''-

(ethane-1,1,1-triyl)tris(4,1-phenylene))tris(oxo) trihexanoate (D-(ENAZ)₃, 4): (*E*)-2-(4-((4-((4-nitrophenyl)diazenyl)phenyl)(phenyl)amino)phenoxy)ethanol, **1** (0.5 g, 1.1 mmol), 6,6',6''-(4,4',4''-(ethane-1,1,1-triyl)tris(4,1-phenylene))tris(oxo)trihexanoic acid, **3** (0.22 g, 0.33 mmol), and 4-(dimethylamino)-pyridium-4-toluene sulfonate (DPTS) (0.26 g, 0.89 mmol) were mixed in 20 mL of CH_2Cl_2 under argon at room temperature. *N,N'*-dicyclohexylcarbodiimide (DCC, 0.45 g, 2.2 mmol) was added and the reaction mixture was stirred for 24 h. The reaction mixture was filtered to remove resultant urea. After concentrating into a minimum volume of solution, it was added into methanol for collecting solid precipitates. The resulting product was purified by silica gel column chromatography (EtOAc/ $\text{CHCl}_3 = 1:20$) to yield 0.5 g (77.4%) of a red solid. T_g 70 °C.

$^1\text{H NMR}$ (400 MHz, CDCl_3) δ (ppm): 1.46-1.54 (m, 6H), 1.68-1.81 (m, 12H), 2.06 (s, 3H), 2.40 (t, $J = 7.4$ Hz, 6H), 3.90 (t, $J = 6.4$ Hz, 6H), 4.18 (t, $J = 4.8$ Hz, 6H), 4.45 (t, $J = 4.8$ Hz, 6H), 6.75 (d, $J = 8.4$ Hz, 6H), 6.90-6.96 (m, 12H), 7.02 (d, $J = 8.8$ Hz, 6H), 7.11-7.18 (m, 15H), 7.30-7.34 (t, $J = 7.8$ Hz, 6H), 7.82 (d, $J = 9.2$ Hz, 6H), 7.95 (d, $J = 9.2$ Hz, 6H).

8.34 (d, $J = 8.8$ Hz, 6H).

Elemental Analysis Calcd. for $C_{116}H_{108}N_{12}O_{18}$: C, 71.15%; H, 5.56%; N, 8.58%. Found: C, 71.04%; H, 5.16%; N, 8.63%.

MALDI-TOF: Found: 1958.41 [m]⁻ (calcd. for $C_{116}H_{108}N_{12}O_{18}$: 1958.17).

Synthesis of Tris(2-(5-(diphenylamino)-2-((E)-(4-nitrophenyl)diazenyl)phenoxy)ethyl)-6,6',6''-(4,4',4''-(ethane-1,1,1-triyl)tris(4,1-phenylene))tris(oxy)trihexanoate (D-(SNAZ)₃, 4): (E)-2-(5-(diphenylamino)-2-((4-nitrophenyl)diazenyl)phenoxy)ethanol, 2 (0.37 g, 0.82 mmol), 3 (0.17 g, 0.25 mmol), and DPTS (0.19 g, 0.66 mmol) were mixed in 20 mL of CH_2Cl_2 under argon at room temperature. DCC (0.20 g, 0.98 mmol) was added and the reaction mixture was stirred for 24 h. The reaction mixture was filtered to remove resultant urea. After concentrating into a minimum volume of the solution, it was added into methanol for collecting solid precipitates. The resulting product was purified by silica gel column chromatography (EtOAc/ $CHCl_3 = 1:20$) to yield 0.4 g (81.8%) of a red solid. T_g 68 °C.

¹H NMR (300 MHz, $CDCl_3$) δ (ppm): 1.38-1.48 (m, 6H), 1.60-1.74 (m, 12H), 2.06 (s, 3H), 2.33 (t, $J = 7.5$ Hz, 8H), 3.82 (t, $J = 6.3$ Hz, 8H), 4.19 (t, $J = 4.7$ Hz, 8H), 4.47 (t, $J = 4.7$ Hz, 8H), 6.59-6.63 (m, 6H), 6.71 (d, $J = 8.7$ Hz, 6H), 6.94 (d, $J = 9.0$ Hz, 6H), 7.14-7.19 (m, 18H), 7.34 (t, $J = 8.1$ Hz, 12H), 7.70 (d, $J = 9.6$ Hz, 3H), 7.95 (d, $J = 9.0$ Hz, 6H), 8.33 (d, $J = 9.0$ Hz, 6H).

Elemental Analysis Calcd. for $C_{116}H_{108}N_{12}O_{18}$: C, 71.15%; H, 5.56%; N, 8.58%. Found: C, 71.13%; H, 5.08%; N, 8.42%.

MALDI-TOF: Found: 1958.29 [m]⁺ (calcd. for $C_{116}H_{108}N_{12}O_{18}$: 1958.17).

Characterization.

Instrumental Analysis: ¹H NMR spectra were recorded on a Varian Mercury NMR 300 Hz spectrometer using deu-

terated chloroform purchased from Cambridge Isotope Laboratories, Inc. Elemental analyses were performed by the Center for Organic Reactions using an EA1112 (Thermo Electron Corp.) elemental analyzer. Thermal properties were studied under a nitrogen atmosphere on a Mettler DSC 821^e instrument.

Film Fabrication: The star-shaped molecules were dissolved in THF for film fabrication. The 5 wt% polymer solutions were filtered with 0.2 μm disc type syringe filters and then spin-coated onto glass slides or quartz plate. The films were dried in a vacuum oven at 60 °C for 48 h.

Formation of the Surface Relief Grating: The gratings on the films were recorded under ambient conditions with the interference pattern produced by a linearly p-polarized Argon ion laser at 514 nm (LEXEL, 1W). Figure 1 shows the two-beam interference setup for this experiment. $\pm 45^\circ$ polarized laser beams were used to be coupled on the film surface. The angle between two beams is approximately 28°. Two writing beams with equal intensities (0.1 mW/cm²) were crossed in the sample film and produced the interference pattern with fringe spacings. A linearly polarized He-Ne laser light ($+45^\circ$, $\lambda = 633$ nm) with weak intensity (1 mW) was used as a probe beam. The grating formation was monitored by measuring the intensity of the first-order diffracted light. The diffraction efficiency, η was simply determined by the ratio of intensities of the incident probe and the diffracted beam.

Results and Discussion

Synthetic procedure of three-armed star-shaped molecules is depicted in Scheme I. (E)-2-(4-((4-nitrophenyl)diazenyl)phenyl)(phenylamino)phenoxy ethanol (1) and (E)-2-(5-(diphenylamino)-2-((4-nitrophenyl) diazenyl)phenoxy)-

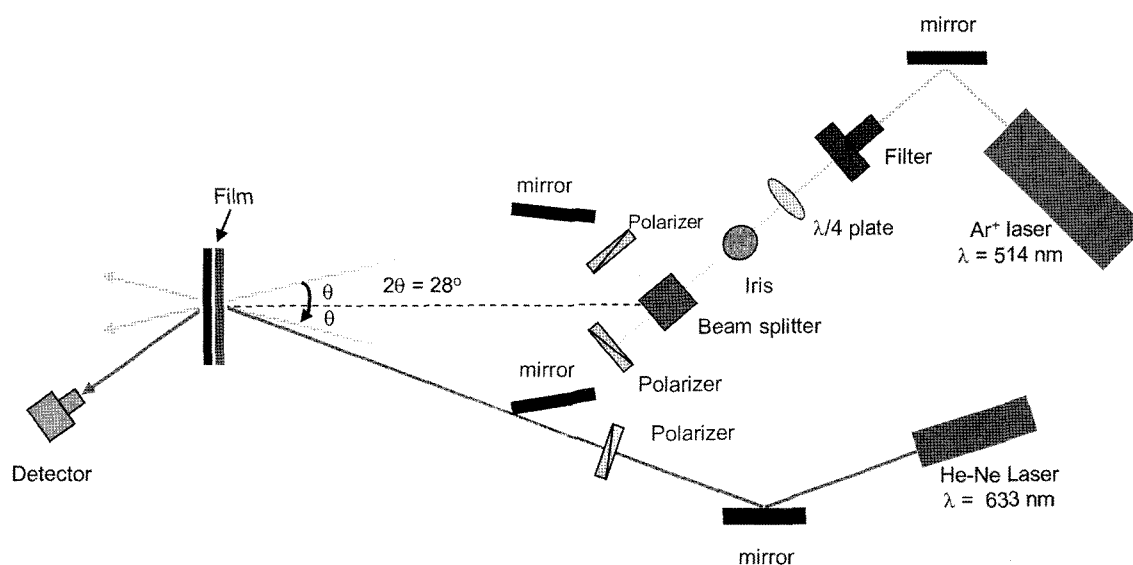


Figure 1. Experimental setup for measuring the intensity of the 1st order diffracted light.

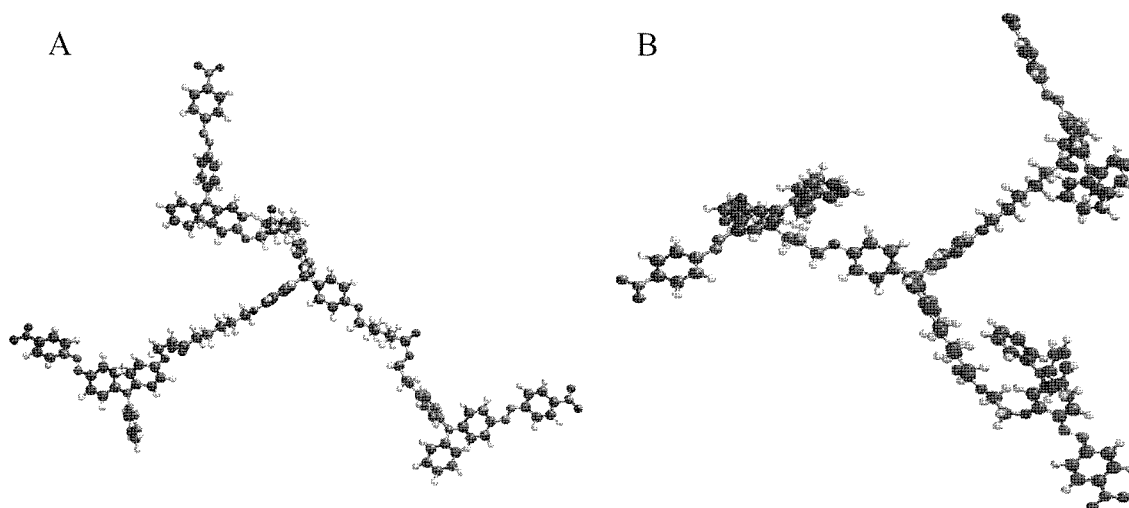


Figure 2. Optimized geometries of three-armed star-shaped molecules. (A) **4** and (B) **5**.

ethanol (**2**) were attached to 6,6',6''-(4,4',4''-(ethane-1,1,1-triyl)tris(4,1-phenylene)) tris(oxy)trihexanoic acid (**3**) through DCC catalyzed esterification in the presence of DPTS. Resulting white dicyclohexyl urea was completely removed by reprecipitation into tetrahydrofuran (THF). It should be noted that the azobenzene chromophores occupied more than 60% of the mass of the synthesized large molecule.

Two molecules (**4** and **5**) are red in color and well soluble in organic solvents such as THF, dimethylformamide, chloroform, acetone etc. The glass transition temperatures of the molecules were determined to be around 70 °C (**4**) and 68 °C (**5**), which are almost identical together.

The dipole moment of 4-(*N,N*-diphenyl)amino-4'-nitroazobenzene was calculated to be 7.023 in the ground state and the geometry was optimized by using a PC-software (Spartan '06). As we expected, **4** shows extended structure of azobenzene moiety to the outer periphery. **5** has azobenzene moieties that are almost perpendicular to the connecting group in the core unit (see Figure 2). Therefore, the

azobenzene chromophores in **5** are tethered to the core unit as a rotational axle. It seems that the reorientation of the molecule is easier than that in **4**.

The absorption spectra of **4** and **5** are shown in Figure 3 in solution and film states. The maximum absorbances of two molecular films were observed at the identical wavelength of around 492 nm, which are assigned to a π - π^* transition of the *trans*-azobenzene chromophore moiety.

In order to achieve a large diffraction efficiency, the concentration of azobenzene chromophores in materials should be as high as possible. However, in the case of azobenzene-containing homopolymer or copolymer, we cannot avoid the molecular aggregation in the solid state. In our previous study,²¹ we investigated the effect of molecular aggregation on the photoinduced anisotropy in polymethacrylate bearing an aminonitroazobenzene moiety. The absorption spectrum of the polymer is blue-shifted (λ_{max} =420 nm) and the shape of the spectrum is highly skewer than that of solution spectrum (λ_{max} =480 nm). Compared to the aggregation behavior

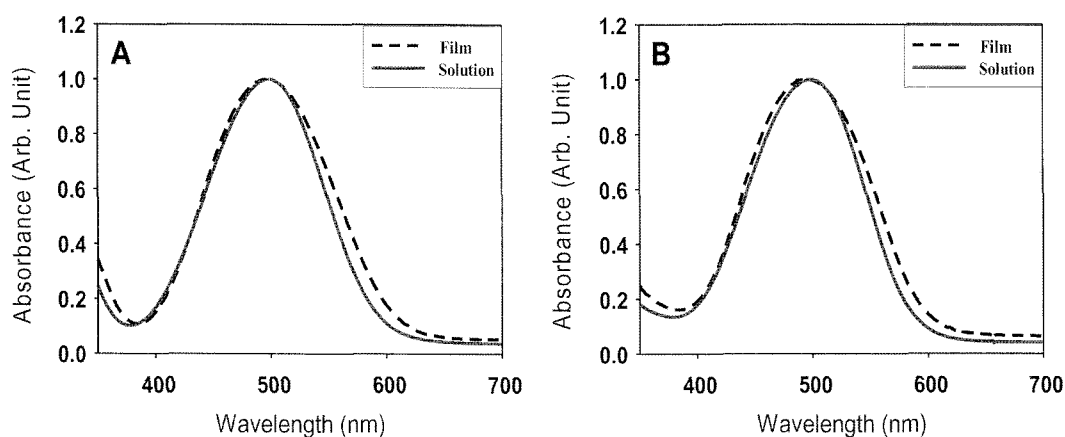


Figure 3. UV-Vis absorption spectra of (A) **4** and (B) **5**.

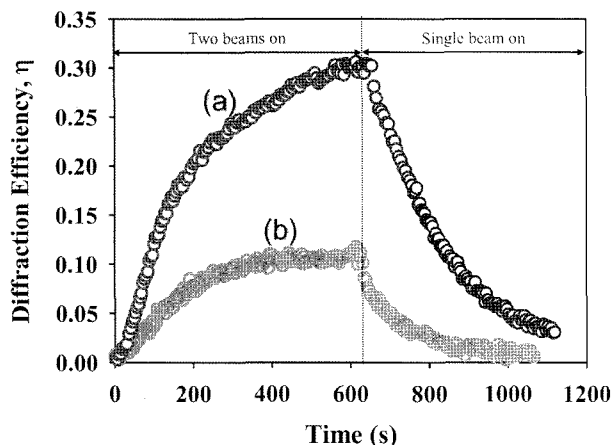


Figure 4. Variation of the diffraction efficiency of (a) **4** and (b) **5**.

of above methacrylate polymer in a film state, three-armed structural molecular design were quite helpful to suppress the molecular aggregation due to an efficient site isolation effect.

Comparison of the Diffraction Behaviors. The holographic recording was well accomplished by two plane waves of 514 nm wavelength with mutually orthogonal polarizations ($\pm 45^\circ$). In this type of writing the resulting light electric field is modulated with intensity and polarization.

We observed that stable diffraction gratings could be fabricated on the present molecular films at room temperature that is well below their T_g s.

The results of SRG experiment in the present molecular samples are shown in Figure 4.

In two molecular films, under the same intensities of two interfered beams, the intensity of the 1st-order diffracted light increased gradually as a function of irradiation time. And then the diffraction efficiency decreased to the lowest level when the linearly polarized single beam ($+45^\circ$) was irradiated. After erasing them by thermal or optical method, they could be recorded again and the almost same value of diffraction efficiency could be achieved even after multiple writing-erasing cycles (> 10 cycles).

As shown in Figure 4, the two experimental rising curves exhibit an initial growth of the diffraction efficiency commonly corresponding to the formation of intensity gratings. The maximum diffraction efficiencies of **4** and **5** were determined to be 31 and 11%, respectively. These values are unusually high, which are rarely observed in amorphous polymers containing similar azobenzene chromophores. This is mainly attributed to very high concentration (ca 60 wt%) of azobenzene chromophore in each star-shaped molecule. In addition, no molecular aggregation in the solid state occurs, which is quite effective to improve the value of a diffraction efficiency.

It is known that the birefringence grating of azo-polymer films, which is attributed to photoinduced alignment of the

Table I. Calculated Parameters of Rising and Decaying Behaviors of the Diffraction Efficiency

| | Rising Curve | | Decay Curve | | |
|----------|--------------|-----------------------------|-------------|--------|-----------------------------|
| | A_0 | $\kappa_1(\text{sec}^{-1})$ | A_1 | A_2 | $\kappa_1(\text{sec}^{-1})$ |
| 4 | 0.3194 | 0.0046 | 0.2963 | 0.0010 | 0.0051 |
| 5 | 0.1144 | 0.0054 | 0.0983 | 0.0115 | 0.0147 |

azobenzene chromophores, is easily erased upon exposure to a single laser beam. Under the single beam irradiation, the reorientation of azo chromophores occurs in a random fashion and the periodicity of the grating diminishes gradually. Besides re-writability and erasability, the dynamic behavior was another issue for fast writing process.

The writing and decaying curves (Figure 4) can be fitted using single exponential functions. The calculated parameters are tabulated in Table I.

The rising curve of a diffraction efficiency was fitted to eq. (1) after turning on the two excitation beams,

$$\eta(t) = A_0(1 - \exp(-k_1 \cdot t)) \quad (1)$$

where A_0 is the amplitude associated with the process having rate constant k_1 , respectively.

Referring to Table I, the rate constant, k_1 is larger for the side-on type molecule, **5**, than that for the end-on type molecule, **4**. The rising rate, k_1 of the diffraction efficiency depends on the quantum yield, the life time of a *cis* chromophore, the rate of photoisomerization, and the mobility of the chromophores in general.

The rate of photoisomerization of the chromophores in the present molecules can be little different from each other, since the modes of their attachment onto the core are different. But the k_1 value reveals a dependence on the structural details of the molecules to some extent. The k_1 value increases slightly from 0.0046 to 0.0054 s^{-1} when the structure of the molecule is changed from **4** to **5**. As far as the dependence of rotational motion of the chromophores on their attachment mode (end-on vs. side-on bonding) to the core is concerned, the diphenyl aminonitroazobenzene chromophore unit in **5** can rotate more easily around the connecting group ($-\text{O}-\text{CH}_2-$) that behaves as a molecular axle than in **4**.

4 shows higher saturated diffraction efficiency ($\eta=0.31$) (Figure 4) than the corresponding values ($\eta=0.11$) for **5** under the low power irradiation ($10 \text{ mW}/\text{cm}^2$), indicating that a higher degree of anisotropic orientation was achieved in the former when compared with the latter. Although the rising rate of **4** is smaller than that of **5**, induction of optical anisotropy and mass transfer of the chromophores in combination with more effective coupling interactions between the chromophores and the core due to their proximity and geometrically more anisotropic orientation might appear to be a major reason for the higher saturation levels for the end-on type molecule. In addition, it can be conjectured that

due to severe geometrical hindrance of a localized free volume in **5**, the overall degree of chromophore alignment is highly limited between the arms although the side-on attached chromophore is more labile to rotate. It is indirectly evident that even after 10 min irradiation, the diffraction efficiency of **4** shows the tendency to increase continuously without saturation. The film made of **5** showed the saturation behavior of diffraction efficiency at 600 sec irradiation.

The signal data obtained during irradiation of a single beam can be fitted to the following eq. (2).

$$\eta(t) = A_1 \exp(-k_2 t) + A_2 \quad (2)$$

where A_1 is amplitude associated with the process having a rate constant k_2 , respectively (Table I). A_2 corresponds to the residual diffraction efficiency even after long-term optical

erasing. In the present molecules, almost no residual diffraction efficiency was observed after optical erasing process. The fast decay is attributed to the fast randomization of the periodic molecular reorientation.

The magnitude of k_2 is much dependent on the manner how the chromophores are bound to the core, i.e., side-on vs edge-on attachment. The side-on attached star-shaped molecule shows slightly higher k_2 values, which is the same tendency observed in the rising curve.

Atomic Force Micrographs of the Surface of Photopolymers. Finally, we observed the surface of the film after recording SRGs by AFM. AFM images of the **4** and **5** were taken after recording the grating at room temperature as shown in Figure 5. The exposure intensity is 14.2 mW/cm² for two molecular films.

First, we irradiated the two linearly polarized lights at cer-

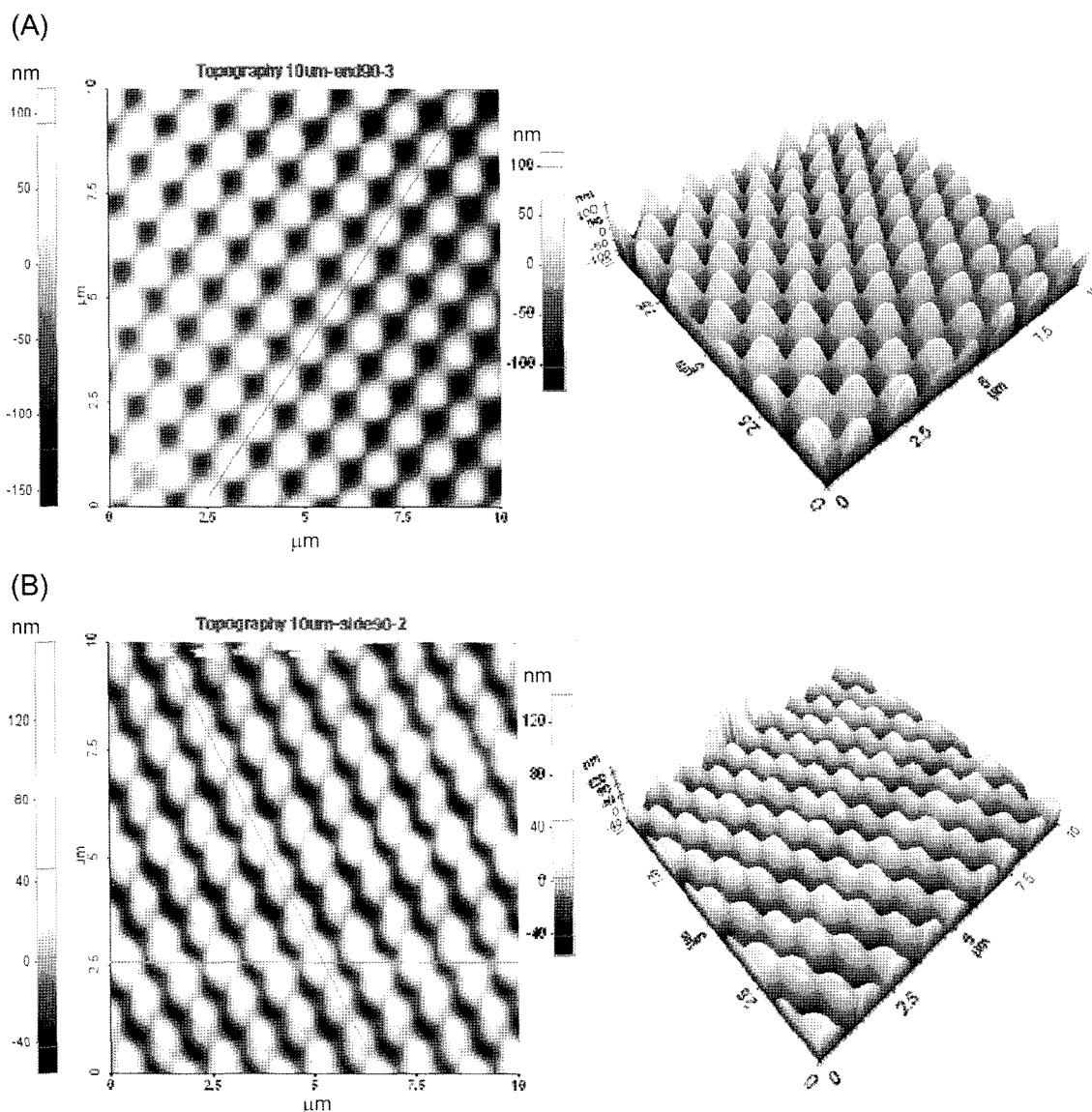


Figure 5. AFM images of the island type grating for light diffusion. (A) **4** and (B) **5**.

tain incidence angle. Then, we rotated the sample by 90° for inscribing orthogonal grating to the first one. Well defined island type 2-dimensional gratings were elaborated. The depth of modulation is 120.6 nm and the period of the grating is 1.13 μm . The theoretical value for the period of the grating is 1.09 μm , so the experimental periodicity of the grating fits well to the theoretical one. It is obvious that our star-shaped molecules exhibit relatively deep modulation depth compared to the conventional azobenzene-containing polymers (ave. depth ~50-80 nm in polymethacrylate bearing azobenzene moieties). We are making much effort to study different kinds of modulation grating with the polarization states of the pumping lights using the new star-shaped molecules or dendrimers.

Conclusions

We have prepared two star-shaped molecules bearing azobenzene-chromophores and studied their dynamic properties of the diffraction efficiency at room temperature. The two molecules differ in the mode of attachment of the chromophores: The chromophores in **5** are bound to the core laterally or side-on attached and the chromophores in **4** perpendicularly or end-on attached. These two molecules reveal fast periodic molecular reorientation of chromophores and optical erasing behaviors at room temperature, which is far lower than their T_g s.

The side-on type molecule, **5** showed faster writing rate than the end-on type molecule, **4**. Such a fast response of the chromophores to the polarized light appears to be due to high mobility of the chromophore units brought about by the low, local rotational energy barriers for the core and the pendants. Just like conventional side chain polymers, side-on attachment of the chromophores renders a higher degree of rotational freedom than end-on attachment, which, in turn, results in a faster response to the polarized light. It should be noted that the star-shaped molecules containing 60 wt% of azobenzene chromophores did not show any trace of molecular aggregation and exhibited unusually high diffraction efficiency. Under our simple synthetic strategy, well site isolation of the chromophores could be achieved to facilitate the rotational motion and displacement of azobenzene molecules at ambient conditions.

Acknowledgment. This work was supported by the Seoul R&BD Program (2007-2008) and NBIT program (MOST and AFOSR, 2007-2008).

References

- (1) T. Ikeda, S. Horiuchi, D. B. Karanjit, S. Kurihara, and S. Tazuke, *Macromolecules*, **23**, 42 (1990).
- (2) C. Chen, L. Dalton, L. Yu, Y. Shi, and W. Steier, *Macromolecules*, **25**, 4023 (1992).
- (3) H. Ringsdorf and H-W. Schmidt, *Makromol. Chem.*, **185**, 1327 (1984).
- (4) V. P. Pham, T. Galstyan, A. Granger, and R. A. Lessard, *Jpn. J. Appl. Phys.*, **36**, 429 (1997).
- (5) P. Rochon, J. Gosselin, A. Natansohn, and S. Xie, *Appl. Phys. Lett.*, **60**, 6 (1992).
- (6) I. Naydenova, L. Nikolova, T. Todorov, N. C. R. Holme, P. S. Ramanujam, and S. Hvilsted, *J. Opt. Soc. Am. B*, **15**, 1257 (1998).
- (7) T. Todorov, L. Nikolova, and N. Tomova, *Applied Optics*, **23**, 4588 (1984).
- (8) L. Nikolova, T. Todorov, M. Ivanov, F. Andruzzi, S. Hvilsted, and P. S. Ramanujam, *Applied Optics*, **35**, 3835 (1996).
- (9) I. Naydenova, Tz. Petrova, N. Tomova, V. Dragostinova, L. Nikolova, and T. Todorov, *Pure Appl. Opt.*, **7**, 723 (1998).
- (10) T. S. Lee, D. Y. Kim, X. L. Jianga, L. Lia, J. Kumap, and S. Tripathy, *Macromol. Chem. Phys.*, **198**, 2279 (1997).
- (11) O. Watanabe, M. Narita, T. Ikawa, and M. Tsuchimori, *Polymer*, **47**, 4742 (2006).
- (12) J. Gao, Y. He, F. Liu, X. Zhang, Z. Wang, and X. Wang, *Chem. Mater.*, **19**, 3877 (2007).
- (13) Y. Wu, A. Natansohn, and P. Rochon, *Macromolecules*, **34**, 7822 (2001).
- (14) M. Han, S. Morino, and K. Ichimura, *Macromolecules*, **33**, 6360 (2000).
- (15) L. Andruzzi, A. Altomare, F. Ciardelli, R. Solaro, S. Hvilsted, and P. S. Ramanujam, *Macromolecules*, **32**, 448 (1999).
- (16) T. K. Lim, S. H. Hong, M. Y. Jeong, G. J. Lee, J. -I. Jin, and H. Y. Oh, *Macromolecules*, **32**, 7051 (1999).
- (17) S. Bai and Y. Zhao, *Macromolecules*, **35**, 9657 (2002).
- (18) Y. Wu, A. Natansohn, and P. Rochon, *Macromolecules*, **34**, 7822 (2001).
- (19) M. Devereux and P. L. A. Popelier, *J. Phys. Chem. A*, **111**, 1536 (2007).
- (20) S. W. Cha, D. H. Choi, D. K. Oh, D. Y. Han, C. E. Lee, and J.-I. Jin, *Adv. Func. Mater.*, **12**, 670 (2002).
- (21) B. J. Kim, S. Y. Park, and D. H. Choi, *Bull. Korean Chem. Soc.*, **22**, 2712 (2001).